Raman spectroscopic and SEM/EDXS analyses of high translucent Nantgarw porcelain

Philippe Colomban, Howell G.M. Edwards, Charles Fountain

Raman Spectroscopic and SEM/EDXS Analyses of high translucent Nantgarw Porcelain

Philippe Colomban [1*], Howell G.M. Edwards [2] and Charles Fountain [3]

[1] Sorbonne Université, CNRS, MONARIS UMR8233, 4 Place Jussieu, 75005, Paris, France.

[2] School of Chemistry and Biosciences, Faculty of Life Sciences, University of Bradford, Bradford ,,West Yorkshire BD18 4JX, United Kingdom.

[3]Nantgarw China Works Museum, Nantgarw House, Tyla Gwyn, Nantgarw CF15 7TB, Glamorganshire, United Kingdom.

*Author for correspondence: philippe.colomban@upmc.fr

Abstract

In the first quarter of the 19th Century the factory established at Nantgarw created some of the finest quality porcelain in the world, rivalling that of Sevres, but beset by economic difficulties resulting from extraordinarily high kiln losses approaching 90%, the production which started in 1817 (ceased by 1820) produced the finest translucency ever achieved in Georgian porcelains. An opportunity has arisen to analyse rare Nantgarw porcelain shards excavated archaeologically from the Nantgarw China Works site. Two types of compositions, bone china and silica-rich pastes are identified by Raman and SEM-EDXS analyse, confirming some ancient studies. The spectral data from "sagged" silica-rich shards are interpreted to reveal potential explanations of the manufacturing fault which significantly contributed to the demise of the ceramics factory. Finally, the pigments and glaze used in Nantgarw porcelain decoration have been analysed and identified for the first time.

Keywords: A: Excavation; B: Nantgarw ; C: Translucency ; D : *Raman spectroscopy*: E: *composition,*

1. Introduction

The output from the Welsh porcelain factory at Nantgarw (*ca.* 1817-1820) was much in demand by a discerning clientele and patrons who held its superb translucency and decoration in the highest esteem (1,2,3,4,5): an example of the highest quality porcelain from Nantgarw is shown in Figure 1, which illustrates its superb translucency and applied enamelled floral decoration. Unfortunately, the appallingly high kiln losses of up to 90% experienced at Nantgarw was not commercially viable and resulted in the demise of the factory by 1820. Auctions of the residual stock decorated locally by Thomas Pardoe from 1821-1823 saw porcelain manufacture cease forever in South Wales, but for a short time the porcelains from Nantgarw held a supremacy over all others in Regency Britain and rivalled imports from the long-established prime Sevres porcelain manufactory in France. Today, collectors still desire the china products of Nantgarw and they command premium prices at auction for their quality and rarity. A background to the establishment of the factory, which was the brain-child of the enigmatic William Billingsley and his kiln manager and his son-in-law, Samuel Walker, involves the geographical sourcing of their raw materials, which had necessarily to be of the very highest quality, the preparation of the body composites and problems associated with the manufacture and distribution of the finished products in an era before the essential railway and road networks generated by the Industrial Revolution in the United Kingdom became operational (6,7,8). A survey of the problems facing the start-up venture at Nantgarw by William Billingsley, Samuel Walker and their financier, William Weston Young, and the overcoming of these difficulties is beyond the scope of this paper but a holistic appreciation has been given in the latest text to emerge on the Nantgarw factory (4).

The importation of vast quantities of Chinese *hard paste* porcelain into Europe in the 16th, 17th and 18th Centuries created an almost insatiable desire for this new material which saw the establishment of a competitive European market through the formation of porcelain

manufactories (for a list of the important contributors in this time frame, see Edwards (9)): after a few trials in the manufacture of porcelain, especially at Rouen and St. Cloud in France towards the end of the 17th Century (10,11,12,13,14,15,16), the first creditable commercial production of hard-paste porcelain occurred at Meissen in 1708, where Ehrenfriede Walther von Tschirnhaus and Johann Bottger, with the support of Augustus, Elector of Saxony, made a type of porcelain (15,17) which was, however, chemically and compositionally unlike its Chinese analogue, known thereafter as "true" porcelain (12,15,16,17). Analytical chemical science was still then in its infancy and it was only in 1725 when Father Francois Xavier d'Entrecolles, a Jesuit missionary in Jingdezhen, China, discovered the secrets of Chinese porcelain composition and manufacture which he transmitted to his superiors in France (18) that European factories could commence a serious and competitive porcelain production. R.-A. Ferchault de Réaumur published the first analytical studies of porcelain from 1716 to 1729 (19). The role of kaolin, or China clay, was not appreciated initially and in the interim a *soft paste* porcelain variety was manufactured in Europe which was compositionally different from the Chinese *hard paste* variety but rather linked to Iznik fritware (14,20), but this was much admired for its ability to take a good enamelling decoration. The discovery of localised deposits of China clay in Saxony (17), in France (16) and in Cornwall in the 1730s and 1740s (4,9,10) further encouraged the growth of porcelain manufacture and the establishment of factories which produced *soft paste* (kaolin free, adding a frit to weld quartz grains) and then *hard paste* (i.e. using kaolin) porcelains (9). The quest for better translucency of the china depended very much upon two aspects: conformity and quality control of the raw materials used in the porcelain paste and artefact production and a much stricter control of the kiln design and hence of the homogeneity of the firing temperatures. To achieve the former, novel additives were empirically adopted in the porcelain mixtures before firing, and for the latter, greater attention was applied to the kilns and their operation to reduce wastage upon firing.

At this stage, the complex solid state reactions that occurred in the porcelain paste mixtures at high temperatures in the kilns were not understood chemically and improvements to the ceramic products depended on empirical changes being made in composition and firing: Simeon Shaw (9) was probably the first to attempt to describe porcelain manufacture from a scientific approach and earlier records of changes in body composition are clearly practical but empirical, such as those noted by Dillwyn (21) at Swansea between 1815 and 1817.

Hitherto, the analyses of porcelains have invariably involved the complete or partial destruction of specimens to engage firstly with wet chemical analytical methods and, more recently, the removal of small samples for elemental analytical instrumentation procedures to be undertaken (22). A major advantage of Raman spectroscopy and SEM/EDXS for the analysis of ceramic shards excavated archaeologically at the abandoned Nantgarw China works site is the ability to interrogate the porcelain body to get information in a non-invasive way on the elemental and molecular composition of the body and its associated glaze with any residual pigment used in decoration (12). The Raman analyse can be performed on-site where rare artefacts are conserved in secure room (14,15,20). This is the first time that Raman spectral data have been reported for Nantgarw porcelains and their interpretation along with supporting SEM/EDXS measurements has provided much novel information about the processes utilised some 200 years ago when this factory was at the pinnacle of its production. Raman spectroscopy has previously been used successfully to interrogate European and Chinese porcelains and faience, including a Rockingham porcelain table-top dating from 1835-1840 (23) and early European ceramics (12-16,24-28).

Previous analytical work

The first detailed chemical analysis of Nantgarw porcelain was carried out by Eccles and Rackham (29) in 1922, who analysed two specimens of porcelain from the Victoria and Albert Museum Collection. One of the Nantgarw pieces analysed was especially significant

historically in that it was part of the *Duncombe* service which had been decorated at Nantgarw by William Billingsley and presented to Edmund Edwards, the landlord of the site occupied by the Nantgarw China Works in lieu of rent. The service eventually passed through one of Edwards' daughters by marriage to the Rev. Duncombe of Llandaff, whence it acquired its name. Both of these fine museum specimens were seriously damaged for the destructive sampling required by the wet chemical techniques used in the analyses. An apparently earlier analysis of a specimen of Nantgarw porcelain from the Lady Charlotte Schreiber collection in the Victoria & Albert Museum, South Kensington, London, was claimed by Sir Arthur Church (30) but no chemical compositional data were provided in support of the analysis.

It was in the 1990s when scanning electron microscopy instrumental techniques were first applied to the analysis of Nantgarw porcelains, commencing in 1991 with the work of Tite and Bimson (31) and followed by that of Owen *et al.* (32,33) later in the decade. Tite and Bimson analysed three Nantgarw shards from the British Museum collection and Owen *et al*. fifteen Nantgarw shards and one damaged plate from a collection. A summary of the results achieved in these analyses is given in Table 1; it should be noted that both the wet chemical analyses and the scanning electron microscopy / EDXS data all provide elemental information from the porcelain bodies which must then be related to the components that were used in the porcelain manufacture which are all compromised and changed chemically by the firing process undertaken at temperatures of up to 1400 ^{0}C in the kilns. This is not a straightforward task as the conversion of some raw material components such as bone ash, kaolin, steatite and flints into complex chemical entities occurs upon heating. Whereas Lewis Dillwyn made detailed notes as a chemist of his empirical trials in the attempted perfection and improvement of his porcelain at Swansea during a two years period from 1815-1817 (21), no such recipes were available for William Billingsley and William Weston Young's

operation at Nantgarw, although after the death of William Billingsley it appears that Samuel Walker, his kiln manager, did seemingly reveal the secret Nantgarw recipe to John Taylor who published it in his book *The Complete Practical Potter* in 1847 (34). This recipe for the porcelain body for Nantgarw porcelain as described in the literature is given below:

26 lbs bone ash, 14 lbs of Lynn sand and 2 lbs potash were mixed with water then made into bricks and fired in a biscuit kiln. Then the 42 lbs of cooled frit was ground with 20 lbs of china clay and made into the paste for firing.

Raman spectroscopy combined with SEM/EDXS elemental analyses is here used to characterise several specimens Nantgarw porcelain using shards from archaeological excavation of the factory site to provide answers to the following questions:

- What elements are present in fired Nantgarw china and are these compatible with the suggestions made for the raw materials used?
- Is there evidence for a single body composition or that of several bodies for the narrow datelines of production?
- Does the composition of a sagged Nantgarw shard indicate the source of the production problem?
- What mineral pigments were used for the decoration of Nantgarw porcelain?

In the light of the previous analytical work which was necessarily destructive to the specimens involved and which was accomplished using mainly shards from factory waste dumps, there is obviously a pressing need for the application of a non-destructive analytical technique which can be utilised on perfect, finished porcelain articles to identify their porcelain bodies through the applied glaze. Raman spectroscopy could address this requirement and was, therefore, used here to characterise Nantgarw porcelain using shards to verify that the presence of the glaze on the finished specimen does not compromise the

recording of the spectral data of the underlying body. If the studies of the shards cited here prove satisfactory the next stage would be the Raman spectroscopic interrogation of perfect and rare Nantgarw porcelain specimens.

2. Experimental

2.1.Specimens

The following specimens, glazed or not (Figure 2), were supplied by the Nantgarw China Works Museum Trust for comparative analytical purposes: comprising a group of shards, glazed and unglazed, excavated from a waste porcelain dump at the Nantgarw China Works site in the 1990s. Several of these exhibited characteristics of the finished Nantgarw china, such as edge mouldings and applied bead decoration (Samples NG1, NG2, NG3 and NG5). One example (NG4) is typical of the so-called "sagged" china, which had warped and distorted significantly at high temperatures in the kiln, so rendering the piece unfit for sale. Three of these, described as NG8 and NG9 (two pieces), are decorated with pigment and shard Nart200 replica is a special comparator from a modern process of re-creation of the antique Nantgarw porcelain from a supposed recipe and emulating experiments which were carried out in the late 19^{th} Century to reproduce this porcelain. The importance of the correlation between waste dump shards and perfect surviving porcelain specimens for the interpretation of the spectral data will become apparent later.

2.2. Raman instrumentation

Raman spectroscopic analyses were carried out using a high sensitivity LABRAM Infinity Dilor spectrometer equipped with a 532nm JDS-Uniphase YAG laser and a HORIBA Jobin-Yvon Peltier cooled CCD to get a global view of the different Raman spectral signatures. The laser power is about 5 mW at the sample. Backscattering measurements are made with

Olympus standard and Long Working Distance x 50 and x 100 objectives. About 10 different spots were analysed for each shard specimen to achieve a representative survey (recording time: 2 to 10 min per spectrum, typically). Complementary measurements have been made with an HR800 HORIBA Jobin-Yvon spectrometer equipped with similar CCD detector but using a blue laser line (488 nm, Coherent Innova 90C Ar^+ ion laser) using variable microscope objectives (x10, x50 and X100 Olympus LMPlan). Both green and blue excitations are well suited for examination of porcelain. Blue laser clean better the porcelain surface and help to get a good spectrum of glaze. It was found advantageous to cut the shards with a diamond saw (Minitom, Struers) and to further break the shard with pliers to have a fresh fracture, observed with a BX51 Olympus Microscope, for the Raman analyses. Polishing liquid residues and pollution from the burial environment can generate a strong fluorescence which is detrimental to Raman analyses; therefore, the shards were thoroughly washed with water before and after the cutting. However, most of the fluorescence observed on laser excitation of the shards arises from the biological film which has developed during their burial in the soil. A few $mW/\mu m^2$ green or blue laser illumination is usually sufficient to clean the surface from this biological film, hence decreasing or eliminating (most of) the fluorescence background. Data interpretation was accomplished through comparison with literature values for key molecular mineral components in the porcelain paste (12,13,14,23,35,36), such as wollastonite, calcium phosphate, quartz, feldspar, anatase, etc.. Accumulated spectral wavenumber and intensity data were not smoothed artificially to remove noise or any emission radiation background and comparisons were effected using spectral stackplots to facilitate the observation of key features and their presence or absence in the spectra of related specimens.

2.3. Elemental composition

Elemental composition of the shards was obtained using a JEOL 5410LV SEM-EDXS spectrometer with an acceleration voltage of 20 kV. In order to limit detrimental charge effects, the sample was partially wrapped with a carbon-rich tape having a window for the area to be analyzed. The charge evacuation is not as good as with the application of a conducting coating (C or Au-Pd) but the samples are better preserved. Furthermore, due to the difficulty of recognizing specific coloured areas on SEM images, the window helps to correlate Raman and SEM-EDXS measurements. EDXS spectra were recorded using a x 400 magnification in order to measure the composition on a submicronic area, similar to that probed by Raman microspectrometry using a x10 objective. It is important to note that, unlike coloured glass, coloured pigment enamels are heterogeneous at the scale of a few microns. Consequently, the mean composition as determined, for example by X-ray fluorescence and other techniques probing a large volume (mm^2), reflect only the mean composition of the specimen. Quantitative elemental analysis (oxide wt%) was achieved using the ZAF calculation method as implemented in the Iridium Ultra software. The validity of the measurements was monitored by applying the same procedure to certified glass-reference samples: "Corning Museum B, C and D" and American "National Bureau of Standard (NBS 620)" and the error is estimated to be less than 10% for most of the measured elements. It should be noted that boron cannot be measured in these experiments.

Transparency was evaluated by illuminating the backside with an optic fibre lighting.

3. Results

3.1. Body analysis

Fig. 3 shows representative spectra recorded on the different shards. Two different signatures are observed, ones characteristics of soft-paste with peak characteristic of wollastonite and calcium phosphate, see further and another with strong quartz signature only, as observed for

hard-paste and some fritwares (12,13,14,15), respectively, are observed: indeed for the NG 6 shard we observe porcelain spectral signature with an intense signature of alpha-quartz (SiO_2), (a strong peak at ~462 cm^{-1} and others weaker at 122, 190, 257, 355, 637, 803 and 1150 cm^{-1} (note the wavenumber are downshifted due to the compressive effect of the other phases as usually observed)(12,36) plus additional broad bands at ~ 490 and 1025 to 1080 cm^{-1}, characteristic of a silico-aluminate glassy phase (24-26) as that observed in hard paste porcelain (12,15). We don't observe mullite signature (refractory mullite is the acicular aluminosicate that forms the nest of needle above 1250°C required to retain the liquid phase and preserve the shape of hard paste porcelain at the top high temperature firing and hence to get a high transparency (37). Mullite phase is hardly detected by Raman scattering due to its very ionic character of Al-O bonds.

For all other shards the typical signature of a soft-paste porcelain with a strong narrow peaks of pseudowollastonite ($CaSiO_3$, ~970, 1080 and 410 cm^{-1}) is obvious. Additionally, in most spectra the signature of calcium phosphate ($Ca_3(PO_4)_2$) is observed (main peak at ~960 cm^{-1}) (Table 2), that is characteristic of bone china (23). Traces of (compressed) quartz are also detected in NG1, NG2, NG3 and NG7 that indicates a significant content of glassy matrix: indeed the mean thermal expansion of glassy aluminosilicate is much lower than that of quartz, which induces compression of the quartz grain on cooling. A large amount of glassy phase and a rather perfect sintering (low porosity) are required to obtain the translucency (Fig. 4). The broad peaks characteristics of the glassy phase are observed at ~450 to 485 and 1080 to 1090 cm^{-1}, the variation indicating different compositions. The main peaks of wollastonite and calcium phosphate are rather close in wavenumber but can be clearly discriminated in NG1, NG4 and NG5. Bands merge more or less into a single peak for NG2, NG3 and NG7, indicating a lower degree of crystallinity and hence a lower temperature of

firing (their translucency is lower, Fig. 4). The best splitting is observed for the Nart200 modern sample; it indicates a higher degree of crystallinity.

Compositions measured by SEM-EDXS are consistent with the Raman spectra (Table 2 and Figure 5). The NG6 composition is richer in silica (80%) and free of phosphorus oxide; the CaO content is also very low; K_2O and Na_2O are measured close to 1.2 and 2.6 %. Alumina content is low (~12.6 %) that is more typical of a fritware than a true hard paste porcelain according usual classification (38). The other compositions are similar, except NG4 which is intermediate (~70 % SiO_2, Fig. 5d). The MgO content is high, 3.1 wt%. NG2, NG3, NG5, and NG8 (as well as for the replica Nart200) show a high P_2O_5 content (15 to 20 wt %) and medium CaO content (10 to 15 % wt). The NG1, NG4 and NG7 shards show a medium P_2O_5 content (4 to 8 wt %, Fig. 5d) and a low CaO content (4 to 10 wt %). The NG2, NG3 and NG8 samples are very similar. The NG2, NG8 and Nart200 specimens exhibit the highest content of phosphorus (18-19 wt %). The carbon doublet (ca. 1350-1600 cm^{-1}) is detected in NG3 and NG5 bodies, indicating that firing has taken place under a reducing atmosphere under conditions required to obtain a white paste in the presence of traces of iron oxide (~0.4 % for NG3 and NG4, 0.3 % or less for the other, traces only for NG1, Table 2), which can be attributed to the impurities of the fine sand used in the mixture.

NG6 and NG4 porcelains have a low amount of flux (P_2O_5+CaO+K_2O+Na_2O+PbO = 4.1 % and 10.9 %, respectively) compared with the other specimens (NG2, NG3, NG5, NG8 and Nart200) which have totals ranging between 21 and 40.1 %. The quality of the sintering is however good (see the translucency in Fig. 4) that indicates that some flux – not measured – has been added, certainly borax (B element not detected by SEM-EDS); addition of bismuth is also possible. Note that these elements are highly volatile and the liquid phase formed can be eliminated during the firing, after they had contributed to the densification. Intermediate

values are measured for the NG1 and NG7 specimens (21 and 16.3 %, respectively). Three groups of porcelain body can hence be identified from the shards:

- The special case of NG6: no phosphorus present and a low flux content measured.
- Specimens NG1, NG4 and NG7 have a low phosphorus content and a low lime content.
- Specimens NG2/NG3, NG5, NG8 and Nart200 have a high phosphorus content.

SEM images show a good sintering of the fired body (Fig. 4). Because of the sagging seen in NG4 caused by overfiring, a large extension of the amorphous phase is observed for the fracture (large smoothed area). Circular pores are observed in many samples (see e.g. for NG5; note the translucency make visible the moulded leave decor by back lighting, Fig. 4) in agreement with a significant amount of liquid phase formed during the sintering step. At high magnification, small crystals can be observed in the amorphous phase, for example in NG1. A very particular microstructure is observed for NG6 silica-rich shard.

3.2. Glaze analysis

Fig. 6 shows the representative spectra obtained of the glaze found on the NG2, NG6 and NG7 specimens. Compositions are given in Table 3. The NG6 glaze shows in some places the signature of diopside (nominal composition $MgSiO_3$) with its characteristic doublet at 660 and 1015 cm^{-1} (14) in agreement with the detection of a significant level of magnesium in the body (3.1 wt %, Table 2) and in the glaze (1.1 wt %, Table 3). The spectra of the NG2 and NG7 specimen glaze show the signature of $Ca_3(PO_4)_2$ with the strong ~960 cm^{-1} peak. The signatures of the glassy (alumino-)silicate (broad band of SiO_4 bending modes at ~450-460 cm^{-1} and stretching band at ~1000 cm^{-1} with a shoulder at ~1155 cm^{-1}) are similar for both the NG2 and NG7 glazes, supported by their similar flux content (Table 3: 10.5 to 13 wt %). The

intensity of the ~1150 cm^{-1} component is higher in the NG6 glaze, in agreement with the higher silica content (Table 3) and expected higher firing temperature.

A well-defined calcium phosphate signature is measured in several places for the NG8 glaze (Fig. 6) although no phosphorus was detected by analysing the glaze surface by SEM/EDXS (Table 3). The high content of phosphorus in the body explains this observation since the body-glaze reaction in the firing kiln leads to a precipitation of calcium phosphate and the larger volume of matter probed by Raman scattering includes the area at the body glaze interphase where calcium phosphate forms. A weak feature is observed at 1400 cm^{-1}, which can tentatively be attributed to the addition of boron, element not detectable by SEM-EDS.

Quartz is observed in the NG9 glaze (458 cm^{-1}, Fig. 6, the lower wavenumber indicating a compressive stress applied by the glaze matrix). Additional peaks at 515 cm^{-1} and 990 cm^{-1} are assigned to undissolved feldspar grains and precipitated wollastonite, due to the Ca-rich body coming into contact with a Ca-poor glaze (Tables 2 & 3).

3.3. Enamel analyses

Figure 6 compares the Raman signatures recorded on the coloured enamels in samples NG8 and NG9. The blue enamel shows the strong ~824 cm^{-1}peak with a 785 cm^{-1} shoulder characteristic of $Na_{0.4}K_{0.1}Ca_{0.5}Pb_4(AsO_4)_3$ lacunar apatite (39) which is usually observed for European 18^{th} century blue enamels made with arsenic-rich cobalt (14) and for some Chinese porcelains (40,41). Both cobalt and arsenic are detected by SEM-EDXS (Table 3). The carbon doublet is also observed. The SiO_4 stretching band has peaks at 985 and 1020 cm^{-1}, in agreement with a mixed lead-alkali glass (42,43). The maroon enamel shows the very characteristic and strong signature of haematite (220-285 cm^{-1} doublet (24-36)) plus the amorphous carbon doublet. The green enamel shows the typical signature of Naples Yellow,

formulated as $PbSn_xSb_{2-x-y}M_yO_{7-d}$, pyrochlore (M= Si, Fe ...), with a strong 135 cm^{-1} peak; the peak at 452 cm^{-1}, stronger than that at 505 cm^{-1} indicates a Sn-rich pyrochlore (44-48). Both Sn and Sb are below the detection limit of our SEM-EDXS analysis. A carbon doublet is also observed here, which indicates that carbon black could have been added as a pigment darkening agent.

As expected, gold is detected in Cassius purple enamel (Table 3). Accordingly a strong fluorescence is observed (Fig. 7) as usual (49). Additionally, in the low wavenumber range the strong intensity of the Lamb modes of Au° nanoparticles increases the Rayleigh wing (50) and led to a very strong carbon doublet (surface resonance enhancement effect). The observation of the carbon doublet for all coloured enamels is consistent with the use of a viscous organic medium or glue to facilitate the adhesion of the enamel precursor onto the already glazed porcelain which is necessitated on account of the absence of porosity of the underlying glaze. A strong band at 1017 cm^{-1} is characteristic of the A_1 stretching mode with associated (F) asymmetric components at 1110, 1124 and 1157 cm^{-1} triplet and a bending asymmetric triplet at 607, 626 and 675 cm^{-1} and symmetric doublet at 415 and 497 cm^{-1}, assignable to unreacted $CaSO_4$ (51). This is consistent with the use of gypsum (or alabaster) as raw material.

4. Interpretation of Results and Comparison with Previous Work

Although SEM/EDXS is useful for the identification of microdomains and elemental distribution in fired ceramics, it must be appreciated that the elemental information obtained from the submicron region interrogation of specimens is naturally of a heterogeneous nature when compared with bulk analyses, such as those obtained from wet chemical analyses exemplified by Eccles & Rackham (29). Also, for the SEM analyses of the porcelain body

freshly fractured shards were required to avoid problems with the surface glaze whereas the Raman spectral data could be also acquired through the transparent glaze and these were found to be identical with those obtained from the glaze-free porcelain body. This result is important for the future Raman spectroscopic interrogation of perfect and glazed porcelain specimens without invasive sampling procedures being contemplated. However the comparison of the data recorded by different teams (Fig. 5) led to the same feature. Several important conclusions can be drawn from the analyses of Nantgarw porcelain shards undertaken in the current work:

- SEM/EDXS data relevant to body oxide composition obtained from the eight antique shards, NG1-NG8, in Table 2 clearly indicate that the Nantgarw porcelain body is composed significantly of silica, alumina, calcium oxide, and phosphate, with minor components of potash, soda, magnesia and haematite giving a total of ~100%. It is to be noted that there is an absence of lead oxide, unlike other porcelains of the 18^{th} and 19^{th} Centuries such as Chelsea which utilised powdered flint glass as an additive to improve the translucency of the fired porcelain body. The presence of the major and minor components is correlated with the mixture of starting materials comprising fine river sand, lime (and/or gypsum), potash, flints, china clay and calcined, and ground bone ash (52). Although flints and sand both contain silica, and china clay (made of kaolin) contains magnesia, alumina and silica only, the only source of phosphorus is calcined bone ash, so the phosphate component is a good measure directly of the percentage of bone ash employed in the raw materials paste. However, as has been pointed out in earlier analytical work on porcelains (4,9,53,54) it is by no means a simple exercise to relate the phosphorus % age determined from the SEM/EDXS determinations to the quantitative percentage of the bone ash component used as raw material in the recipes. The formulation of calcined bone ash, which is chemically calcium phosphate, is dependent upon its sourcing and upon the conditions under which its calcination has taken

place (4,9,53). Furthermore, different analysts gave expressed the elemental phosphorus content determined form their analyses as phosphorus pentoxide (29), phosphoric acid (31) and phosphate (32,33) and these all contain very different amounts of phosphorus per mole or molecular ion. A reasoned attempt to introduce correlation between these different entities has been accomplished by Edwards (4,9) and the earlier data on phosphorus in Table 1 has all been reduced to phosphorus pentoxide to effect a proper comparison to be made of these important data.

- The analytical data presented in the current study in Table 2 are derived from the SEM/EDXS experimental elemental determinations expressed as the appropriate oxides; the values are subject to the individual experimental errors and also to inherent variations such as the local heterogeneity of micro domains and their incompatibility with the mean composition. As highlighted in an earlier assessment (9) the compositional errors afforded by inaccuracies in formulating the recipes, especially variance in the raw materials and the precision of weighing out the individual components also compound the batch to batch variation expected for individual compositional variability. It can be estimated, therefore, that the sum of errors such as these can amount to less than 10 % of an average composition for the body paste mix. Nevertheless, examination of the data in Table 2 and Figure 5 reveals that of the seven ancient shards (NG1-NG3, NG5-NG8) NG6 stands alone in having a significantly higher silica content and NG4 have intermediate composition, with lower alumina and lime and a higher magnesia; the most significant variation between NG6 and the other shards is the extremely low and almost negligible phosphorus content, which means that it is devoid of a bone ash component. The two types of compositions, bone china and silica-rich paste are obvious from the comparison of previous analyses (Figure 5, Table 1), even this point was not highlighted. Historically, there is much evidence that William Billingsley regarded the bone ash component as a vital component of Nantgarw porcelain

(53,54) and he undertook his preparation of the calcined bones and their grinding with the utmost care and deliberation (2,4,8,9). Hence, we should consider the presence of this particular shard as a whiteness of the many experiences made of at Nantgarw to obtain high translucent porcelain.

- Two other shards seem to possess unusually high silica component percentages, namely NG4 and NG7: NG4 is an example of sagged porcelain – items which have lost their integrity of shape in the firing process usually attributed to their reaching excessively high temperatures, termed "overfiring" or having an excess of flux. NG6 and NG7 also have an unusual low translucency when viewed in transmitted light as can be seen in Figure 4. Nantgarw has always been considered to be a soft paste porcelain china but shard NG6 clearly establishes this body as closer to a hard paste classification --- resembling the Chinese porcelain, which contained *petuntse*, a steatitic soapstone, and kaolin but no bone ash. The Raman spectrum of shard NG6 also confirms the absence of a phosphatic component in the 960-980 cm^{-1} region.
- The shard Nart200 from a modern recreation of Nantgarw porcelain using the recipe discussed earlier seems to match that of the original china both in its Raman spectrum and in its elemental oxide compositions: this china shows a texture and a translucency indistinguishable from the original (see on Fig. 4 comparison with NG8 and NG9) and this indicates that the assumed Nantgarw recipe reproduced in Taylor's book (34) is very close indeed to the correct one.

The presence of the "rogue" shard NG6 (NG 4 has an intermediate character between NG6 and 'standard' composition) in those excavated from the waste dump requires explanation. The high quality of translucency, good mechanical strength (experimented with the time required to saw a small piece with a diamond wheel) whatever the high silica content and the

low content of flux (after firing) is strange. Several possibilities can be invoked for its presence there:

- That Billingsley and Walker did in fact attempt to create a new Nantgarw body perhaps to address the high kiln losses experienced in the firing of their paste and by testing addition of borax: a large part of the flux volatilized during the firing leading to a silica-rich body. It is interesting to note that the microstructure of intermediate NG4 sample exhibit a microstructure typical of a glassy phase (Fig. 4) although that of NG6 appears very different. Unfortunately we were not able to detect boron. However, such a drastic step-change from soft paste to bone-free 'hard' paste porcelain would be empirically difficult – in contrast the measured and gradual changes in composition to strengthen his soft paste porcelain instituted by Dillwyn at Swansea in the two years from 1815-1817 and recounted in his work book preserved in the Victoria and Albert Museum (21) would negate the effectiveness of this approach. We can conclude, therefore, that Nantgarw porcelain factory succeeds to fabricate just one body during its production run from 1817 until its closure in late 1819 / early 1820.
- Recent research (9) has identified the possibility of incorporating broken shards from other factories, termed "grog" in the industry, which could be ground up and mixed into a new paste for re-firing in the kilns. Unless these shards were carefully selected, it is a real possibility that significant quantities of hard paste porcelain composite would find its way into a new formulation in admixture with the expected soft paste recipe (It is important to keep in mind that excavated shards are from waste deposit and hence more representative of the tentative and failure than of regular production). Such a procedure would certainly explain the two shard outliers NG4 and NG7, both of which can be seen to be significantly

lower that the remaining shards in lime and phosphorus whilst still having a higher level in silica. Such porcelains could well be re-classified as "hybrid" soft/hard paste in the notation of Eccles and Rackham (29) and similar artefacts appear in his data (Fig. 5).

- A third, but perhaps less likely, scenario would be that following the cessation of porcelain production at Nantgarw by early 1820 the abandoned site was reoccupied some years later and ceramic production re-started: the technical difficulties in undertaking this course would be immense as the original workforce would have been dispersed and the kilns become derelict. However, it is recorded that a descendant of Thomas Pardoe, who decorated the remaining stock of white porcelain remaining at Nantgarw from 1820 until he died in 1823, made a ceramic clay pipes there from about 1835 until they fell out of fashion in the 1880s with the advent of machine-rolled cigarettes. It is unlikely, therefore, that a hard paste shard such as NG6 could have arisen from ceramic clay pipe production. The occurrence of such a rogue shard is not unique in Nantgarw china analysis since Victor Owen *et alia* (32) did note a similar event during their determinations in the late 1990s with shards stored in the British Museum from earlier excavations at the factory site: Owen's data for his shard N4 was remarkably similar to those obtained here – 80.3% SiO_2, 9.1 % Al_2O_3, 0.6% CaO and 0.5% P_2O_5. Later work by Owen & *Morrison* (33) on a different set of Nantgarw shards delivered similar analytical data for shards N25 and N34, giving 80.7and 78.0%, 9.0 and 6.6%, 0.5 and 0.6%, and 0.5 and 0%, respectively, for SiO_2,Al_2O_3, CaO and P_2O_5. Such patterns cannot be fortuitous and further studies need to be carried out comprehensively to seek an answer as to how such "hard paste" porcelain came to be located in the Nantgarw waste dump.

A simple calculation from the advertised Nantgarw recipe indicates that some 43 % of the raw materials was comprised of calcined bone ash: it can be estimated (4,9) that the average percentage of phosphorus pentoxide quoted from our analyses here (using shards NG2 , NG3, NG5, NG8), namely 18.5 %, equates to approximately 44% calcined bone ash – not only in excellent agreement with the figure used in the recipe but also with that obtained from the analytical determination of the modern recreation shard, Nart200.

5. Conclusion

This present study confirms that phosphate-free porcelain prepared at the Nantgarw factory, considered as rogue pieces in a previous series of analyses, can be found among shards excavated at the place of the ancient factory kilns. Furthermore, the identification of such porcelain can be made either by elemental analysis (SEM-EDS) or in a non-invasive way by the identification of the phases by Raman microspectrometry. Thus, future studies works on rare objects assigned to the Nantgarw factory may be possible safely for the objects and in their place of storage with a mobile Raman set-up. The observation of various levels of the P_2O_5/SiO_2 ratio, between 0.3 and 0.45 for 'standard' Nantgarw bone China, free of phosphorus (but with 3 wt % MgO), but also of some other shards with a ratio between 0.05 and 0.15 demonstrates that research to prepare other types of porcelain bodies had probably been made. It was not possible to detect the mullite signature by Raman scattering and the P-free body seems more related to a fritware than hard-paste porcelain. The glaze deposited on the P-free/poor body appears, however, to be similar to those of the standard shards. Transmission Electronic Microscopy is required to classify the material. In addition it is confirmed that the modern replica Nantgarw porcelain body fits perfectly with the standard antique Nantgarw composition.

Acknowledgements

The authors record their appreciation of The Nantgarw China Works Museum Trust, Tyla Gwyn, Nantgarw, for making available a quantity of shards excavated from the site, a selection of which are represented in the analytical work described here.

Figure Captions

Figure 1. Nantgarw porcelain spill vase, ca. 1817-1819, London-decorated with sprays of garden flowers and richly gilded, photographed in transmitted light to illustrate the superb characteristic translucency. *Private collection.*

Figure 2. Group of porcelain shards excavated from the waste dump at the Nantgarw porcelain manufactory.

Figure 3. Raman spectra of porcelain shards: body; bottom, left, Nart200 replica (green laser excitation).

Figure 4: Left, representative SEM photos of the body fracture and right comparison of the body translucency.

Figure 5. Comparison of relative silica, alumina and flux content measured by Eccles&Rackham (29), Tite&Bimson (31) and Owen et al. (32,33) (a), in this work (b) for the body of Nantgarw production and excavated shards, respectively; c) glazes and enamels; d) comparison of the phosphate content expressed as P_2O_5.

Figure 6. Raman spectra of colourless glaze for NG2, NG6, and NG7 porcelain shards: (blue laser excitation)

Figure 7. Raman spectra of coloured glaze for NG8 and NG9 porcelain shards: glaze, overglaze enamels and gilded areas (blue laser excitation)

Tables

Table 1. Previous analytical works.

Table 2. Body compositions

Table 3: Glaze/enamel compositions

References

1. E. Morton Nance, The Pottery and Porcelain of Swansea and Nantgarw, B.T. Batsford Ltd., London, 1942.
2. W.D. John, Nantgarw Porcelain, Ceramic Book Co., Newport, 1948.
3. W. Turner, The Ceramics of Swansea and Nantgarw, Bemrose & Sons, Old Bailey, London, 1897.
4. H.G.M. Edwards, Swansea and Nantgarw Porcelain: A Scientific Reappraisal, Springer Publishing, Dordrecht, The Netherlands, 2017.
5. H.G.M. Edwards, Nantgarw Porcelain: The Pursuit of Perfection, Penrose Antiques Ltd. Short Guides, Series Editor: M.D. Denyer, Penrose Antiques Ltd., Thornton, West Yorkshire, UK, 2017, ISBN : 978-0-244-90654-2.
6. W.D. John, William Billingsley, Ceramic Book Co., Newport, 1968.
7. H.G.M. Edwards and M.C.T. Denyer, William Billingsley. The Enigmatic Porcelain Artist, Decorator and Manufacturer, Penrose Antiques Ltd. Short Guides, Neopubli, Berlin, 2016. ISBN: 978-3- 7418- 6802-3.
8. H.G.M. Edwards, Swansea and Nantgarw Porcelain Bodies Based on Analytical Evidence: A Case Study, in Encyclopaedia of Analytical Chemistry, ed. R. Meyers and Y. Ozaki, J. Wiley and Sons, Chichester, UK, 2015.
9. H.G.M. Edwards, Nantgarw and Swansea Porcelains: An Analytical Perspective, Springer Publishing, Dordrecht, The Netherlands, 2018.
10. I. Freestone, Science and Early British Porcelain, Proceedings of the Sixth Conference and Exhibition of the European Ceramics Society, London, June 1999, International Ceramics Societies, Volume 1, pp.11-17, 2000.
11. D.W. Kingery, D. Smith, The development of European soft-paste (Frit) porcelains, in Ancient Technology to Modern Science, vol. I, Ceramics and Civilization, Kingery D.W. Ed, The Amer. Ceramic Soc., Columbus, OH, 1984**,** pp. 273-292.
12. Ph. Colomban, F. Treppoz, Identification and Differentiation of Ancient and Modern European Porcelains by Raman Macro- and Micro-spectroscopy, J. Raman Spectrosc. 32 (2) (2001) 93-102.
13. Ph. Colomban, I. Robert, C. Roche, G. Sagon, V. Milande, Identification des porcelaines “tendres” du 18ème siècle par spectroscopie Raman: Saint-Cloud, Chantilly, Mennecy et Vincennes/Sèvres, Revue d’Archéométrie, 28 (2004) 153–167.
14. Ph. Colomban, T.-A. Lu, V. Milande, Non-Invasive on-site Raman study of blue-decorated early soft-paste porcelain: the use of Arsenic-rich (European) cobalt ores – Comparison with huafalang Chinese porcelains, Ceram. Inter. 44 (8) (2018) 9018-9026.
15. Ph. Colomban, V. Milande, On Site Analysis of the earliest known Meissen Porcelain and Stoneware, J. Raman Spectrosc. 37 (5) (2006) 606-613.

16. M. Maggetti, A. d'Albis, Phase and compositional analysis of a Sèvres soft paste porcelain plate from 1781, with a review of early porcelain techniques, Eur. J. Mineral. 29 (3) (2017) 347-367.

17. W. Goder, W. Schulle, O. Wagenbreth, H. Walter, La découverte de la porcelaine européenne en Saxe Böttger, J.F. Pygmalion-Gérard Watelet Press, 1984, Paris.

18. A.M. Pollard, Letters from China: A History of the Origins of the Chemical Analysis of Ceramics, AMBIX (Society for the History of Archaeology and Chemistry), **62**, pp. 50-71, 2015.

19. R.A. Ferchault de Réaumur, Observations sur la matière qui colore des perles fausses et sur quelques autres matières animales d'une semblable couleur, à l'occasion de quoi on essaie d'expliquer la formation des écailles de poissons, Mémoires Académie des Sciences, Paris (1716). Idée générale des différentes manières dont on peut faire la porcelaine et quelles sont les véritables matières de celle de la Chine, ibidem (1727). Second mémoire sur la porcelaine ou suite des principes qui doivent conduire dans la composition des porcelaines de différents genres et qui établissent les caractères des matières fondantes qu'on ne peut choisir pour tenir lieu de celle qu'on emploie à la Chine, ibidem (1729). Available at https://www.academie-sciences.fr/pdf/dossiers/Reaumur/Reaumur_publi.htm.

20. Ph. Colomban, V. Milande, L. Le Bihan, On-site Raman Analysis of Iznik pottery glazes and pigments, J. Raman Spectrosc. 35 (2004) 527-535.

21. L.W. Dillwyn, Notes on the Experimental Production of Swansea Porcelain Bodies and Glazes made by Lewis Weston Dillwyn with Samuel Walker at the Swansea China Works between 1815 and 1817 presented to the Library of the Victoria & Albert Museum, South Kensington, London by John Campbell in 1920. Reproduced in Eccles & Rackham, Analysed Specimens of English Porcelain, 1922, see reference 29.

22. Ph. Colomban, The Destructive/Non-destructive Identification of Enameled Pottery, Glass Artifacts and Associated Pigments – a Brief Overview, Arts **2** (2013) 77-110.

23. H.G.M. Edwards, Ph. Colomban, B Bowden, Raman Spectroscopic Analysis of an English Soft-paste Porcelain Plaque-mounted Table, J. Raman Spectrosc. 3**5** () (2004)656-661.

24. Ph. Colomban, G. Sagon, X. Faurel, Differentiation of Antique Ceramics from the Raman Spectra of their Coloured Glazes and Paintings, J. Raman Spectrosc. 32 () (2001) 351-360.

25. Ph. Colomban, Raman Spectrometry: A Unique Tool to Analyze and Classify Ancient Ceramics and Glasses, Appl. Phys. A, 79 (2004) 167-170.

26. Ph. Colomban, A Case Study: Glasses, Glazes and Ceramics, in Raman Spectroscopy in Archaeology and Art History, eds, H.G.M. Edwards and J.M. Chalmers, Royal Society of Chemistry Publishing, Cambridge, 2005.

27. Ph. Colomban, V. Milande, H. Lucas, On-site Raman Analysis of Medici Porcelains, J. Raman Spectrosc. 35 () (2004) 68-72.

28. P. Ricciardi, Ph. Colomban, B. Fabbri, V. Milande, Towards the Establishment of a Raman Database of Early European Porcelain, e-Preserv. Sci.6 (2006) 22- 26.

29. H. Eccles, B. Rackham, Analysed Specimens of English Porcelain in the V&A Museum Collection, Victoria & Albert Museum, South Kensington, London, 1922.

30. Sir A.H. Church, English Porcelain: A Handbook to the China Made in England During the 18th Century as Ilustrated by Specimens Chiefly in the National Collection, A South Kensington Museum Handbook, Chapman & Hall Ltd., London, 1894.

31. M.S. Tite, M. Bimson, A Technological Study of English Porcelains, Archaeometry 33 () (1991) 3- 27.

32. J.V. Owen, J.O. Wilstead, R.W. Williams, T.E. Day, A Tale of Two Cities: Compositional Characteristics of Some Nantgarw and Swansea Porcelains and Their Implications for Kiln Wastage, J. Archaeol. Sci. 25 () (1998) 359-375.

33. J.V. Owen, M.L. Morrison, Sagged Phosphatic Nantgarw Porcelain (ca. 1813-1820): Casualty of Overfiring or a Fertile Paste? Geoarchaeology, 14 (1999) 313-332 .

34. J. Taylor, The Complete Practical Potter, Shelton, Stoke-upon-Trent, 1847.

35. D. Mancini, C. Dupont-Logiè, Ph. Colomban, On-site Identification of Sceaux Porcelain and Faience Using a Portable Raman Instrument, Ceramics Int., 42 () (2016) 14918-14927.

36. Ph. Colomban, M. Maggetti, A. d'Albis, Non-invasive Raman identification of crystalline and glassy phases in a 1781 Sèvres Royal Factory soft paste porcelain plate, J. Eur. Ceram. Soc. 38 (15) (2018) 5228-5233.

37. Ph. Sciau, L. Noé, Ph. Colomban, Metal nanoparticles in contemporary potters' master pieces: Lustre and red "pigeon blood" pottery: Models to understand the ancient technology Ceramics Int. 42 (14) (2016) 15349-15357.

38. A. Brongniart, Traité des arts céramiques ou Des poteries considérées dans leur histoire, leur pratique et leur théorie, Paris, Béchet jeune, A. Mathias, 1844, 3 vols. http://catalogue.bnf.fr/ark:/12148/cb36023945s.public (accessed 21th December 2017). Third edition is more complete : 3rd Edition, avec Notes et Additions par A. Salvetat, P. Asselin–Libraire de la Faculté de Médecine, 2 Vol. Paris, 1877.

39. B. Manoun, M. Azdouz, M. Azrour, R. Essehli, S. Benmokhtar, L. El Ammari, A. Ezzahi, A. Ider, P. Lazor, Synthesis, Rietveld refinements and Raman spectroscopic studies of tricationic lacunar apatites $Na_{1-x}K_xPb_4(AsO_4)_3$ ($0 < x < 1$), J. Mol. Struct. 986 (1-3) (2011) 1–9.

40. J. Van Pevenage, D. Lauwers, D. Herremans, E. Verhaeven,B. Vekemans, W. De Clercq, L. Vincze, L. Moens, P. Vandenabeele, A Combined Spectroscopic Study on Chinese Porcelain Containing Ruan-Cai Colours, Anal. Methods 6 (2) (2014) 387-394.

41. Ph. Colomban, F. Ambrosi, A.-T. Ngo, T.-A. Lu, X.-L. Feng, S. Chen, C.-L. Choi, Comparative analysis of wucai Chinese porcelains using mobile and fixed Raman microspectrometers, Ceram. Int. 43 (16) (2017) 14244-14256.

42. Ph. Colomban, Polymerisation Degree and Raman Identification of Ancient Glasses used for Jewellery, Ceramics Enamels and Mosaics, J. Non-Crystall. Solids 323 (1-3) (2003) 180-187.

43. Ph. Colomban, A. Tournié, L. Bellot-Gurlet, Raman Identification of glassy silicates used in ceramic, glass and jewellry: a tentative differentiation guide, J. Raman Spectrosc. 37 (8) (2006) 841-852.

44. M. Pereira, T. de Lacerda-Aroso, M.J.M. Gomes, A. Mata, L.C. Alves, Ph. Colomban, Ancient Portuguese Ceramic Wall Tiles (Ajulejos): Characterization of the Glaze and Ceramic Pigments, J. Nano Research 8 (2009) 79-88.

45. C. Sandalinas, S. Ruiz-Moreno, A. Lopez-Gil, J. Miralles, Experimental Confirmation by Raman Spectroscopy of a Pb-Sn-Sb Triple Oxide Yellow Pigment in Sixteenth-Century Italian Pottery, J. Raman Spectrosc. 37 (10) (2006) 1146-1153.

46. F. Rosi, V. Manualli, C. Milliani, B.G. Brunetti, A. Sgamellotti, T. Grygar, D. Hradil, Raman Scattering Features of Lead Pyroantimonate Compounds. Part I: XRD and Raman Characterization of Pb2Sb2O7 Doped with Tin And Zinc, J. Raman Spectrosc. 40 (1) (2009) 107-111.

47. C. Pelosi, G. Agresti, U. Santamaria, E. Mattei, Artifical Yellow Pigments: Production and Characterization Through Spectroscopic Methods of Analysis, ePreserv. Sci. 7 (2010) 108-115.

48. Ph. Colomban, L. Arberet, B. Kirmizi, On-site analysis of 17^{th} - 18^{th} centuries Limoges enamels. Arsenic and the technological relationship between enamelled Limoges and Chinese wares, Ceram. Int. 43 (13) (2017) 10158-10165.

49. Ph. Colomban, B. Kirmizi, C. Gougeon, M. Gironda, C. Cardinal, Pigments and glassy matrix of the 17^{th}-18^{th} century enamelled French watches: A non-invasive on-site Raman and pXRF study J. Cult. Herit, in press.

50. G. Simon, L. Meziane, A. Courty, Ph. Colomban, I. Lisiecki, Low wavenumber Raman scattering of cobalt nanoparticles self-organized in 3D superlattices far from surface plasmon resonance, J. Raman Spectrosc. 47 (2) (2016) 248-251.

51. J. Roman-Lopez, V. Correcher, J. Garcia-Guinea, T. Rivera, I.B. Lozano, Cathodoluminescence and green-thermoluminescence response of $CaSO_4$:Dy,P films, J. Luminescence 135 () (2013) 89-92.

52. W.M. Carty, U. Senapatti, Porcelain-raw materials, processing, phase evolution, and mechanical behavior, J. Am. Ceram. Soc. 81 (1998) 3–20.

53. J.V. Owen, A New Classification Scheme for 18^{th} Century American and English Soft Paste Porcelain, in Ceramics in America, ed. R. Hunter, Chipstone Foundation, Milwaukee, Wisconsin, USA, pp. 45-61, 2002.

54. S. Morgulis, E. Janacek, Studies on the Chemical Composition of Bone Ash, J. Biol. Chemistry, **93** (1931) 455-466.

55. M. Hillis, The Development of Welsh Porcelain Bodies, in *Welsh Ceramics in Context*, Part II, ed. J. Gray, Royal Institution of South Wales, Swansea, pp. 170-192, 2005.

FIGURE 1

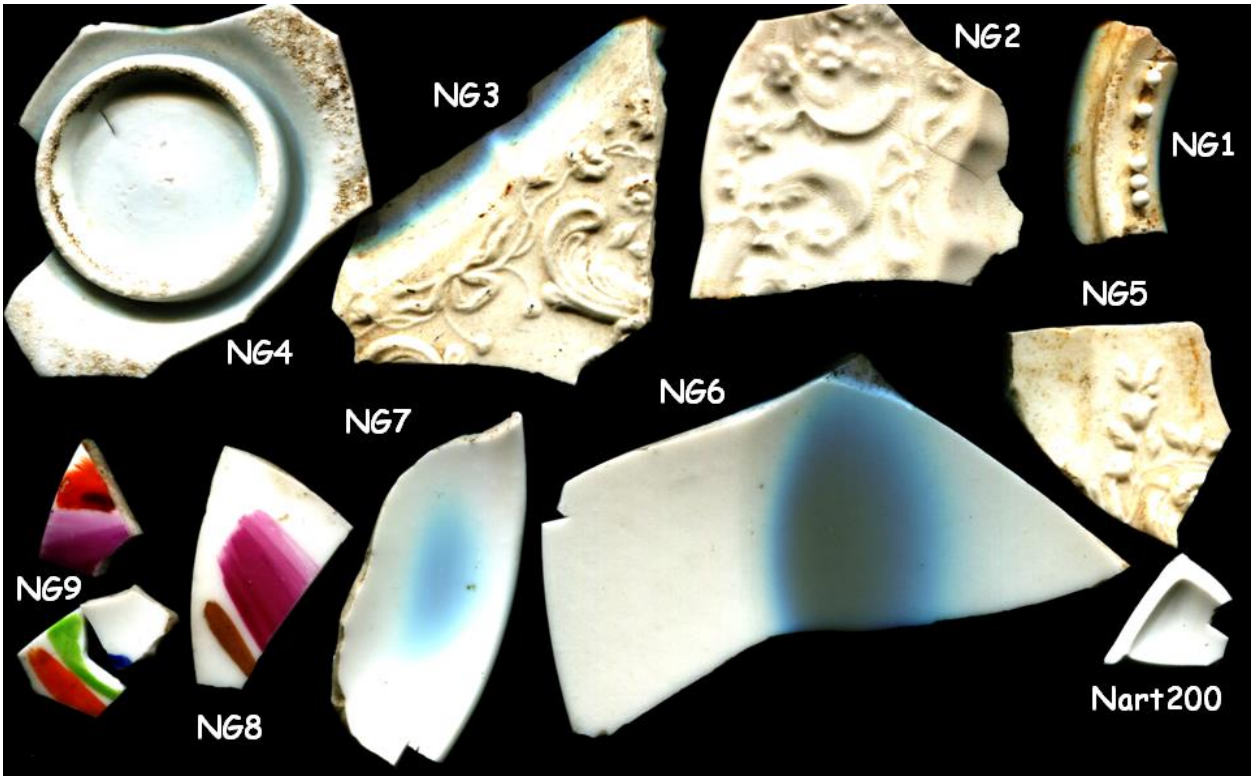

FIGURE 2

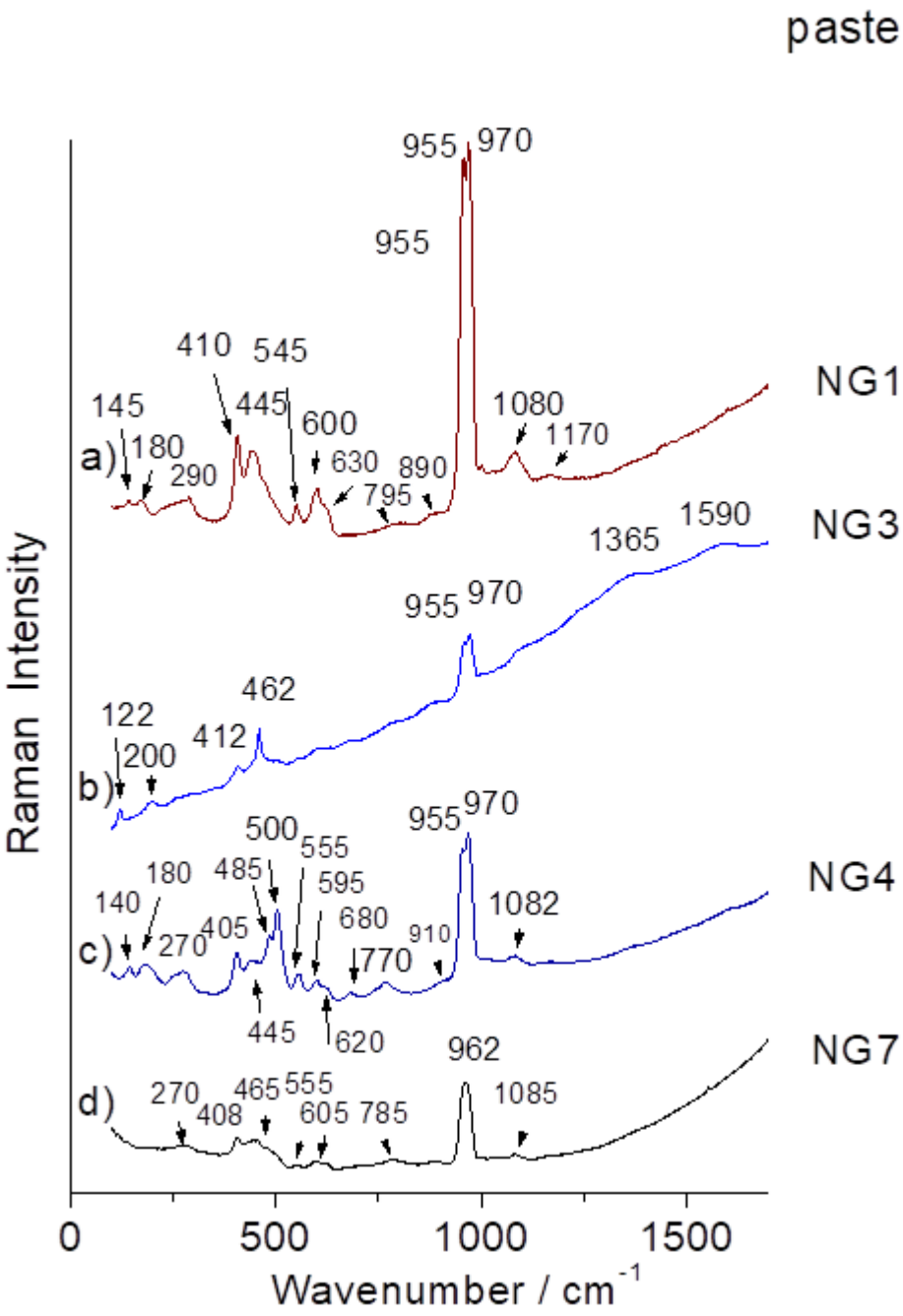

FIGURE 3 LEFT TOP

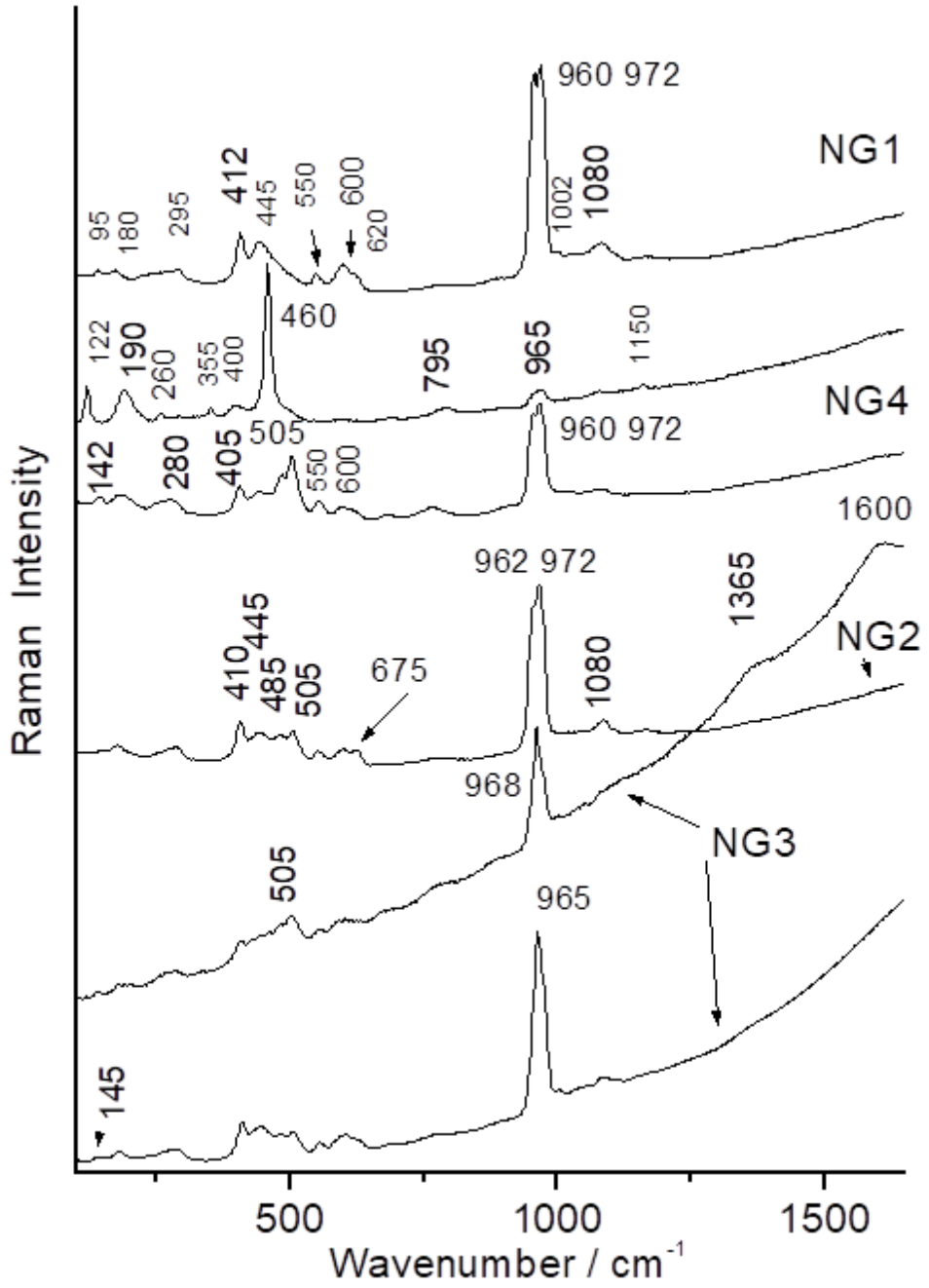

FIGURE 3 RIGHT TOP

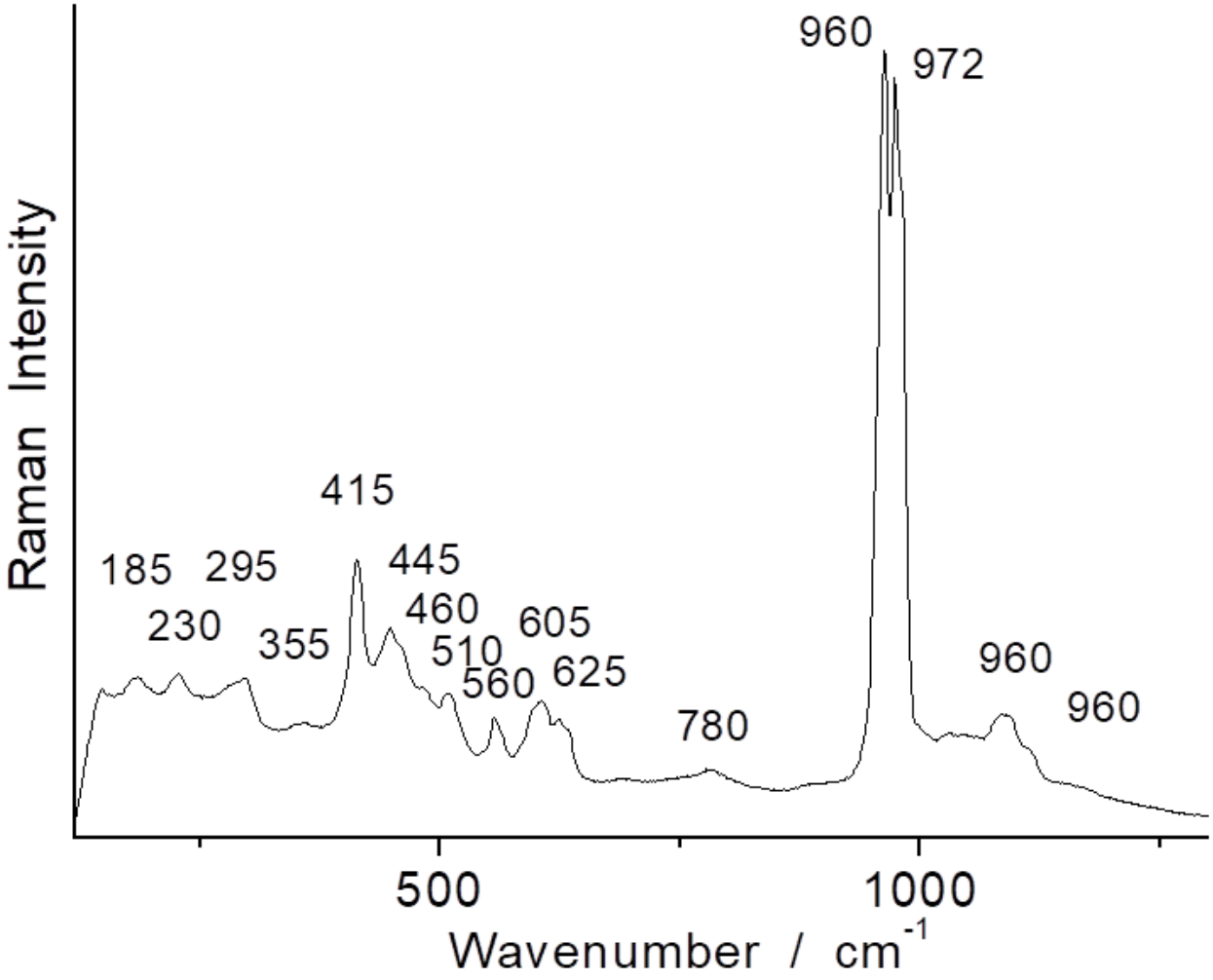

FIGURE 3 LEFT BOTTOM

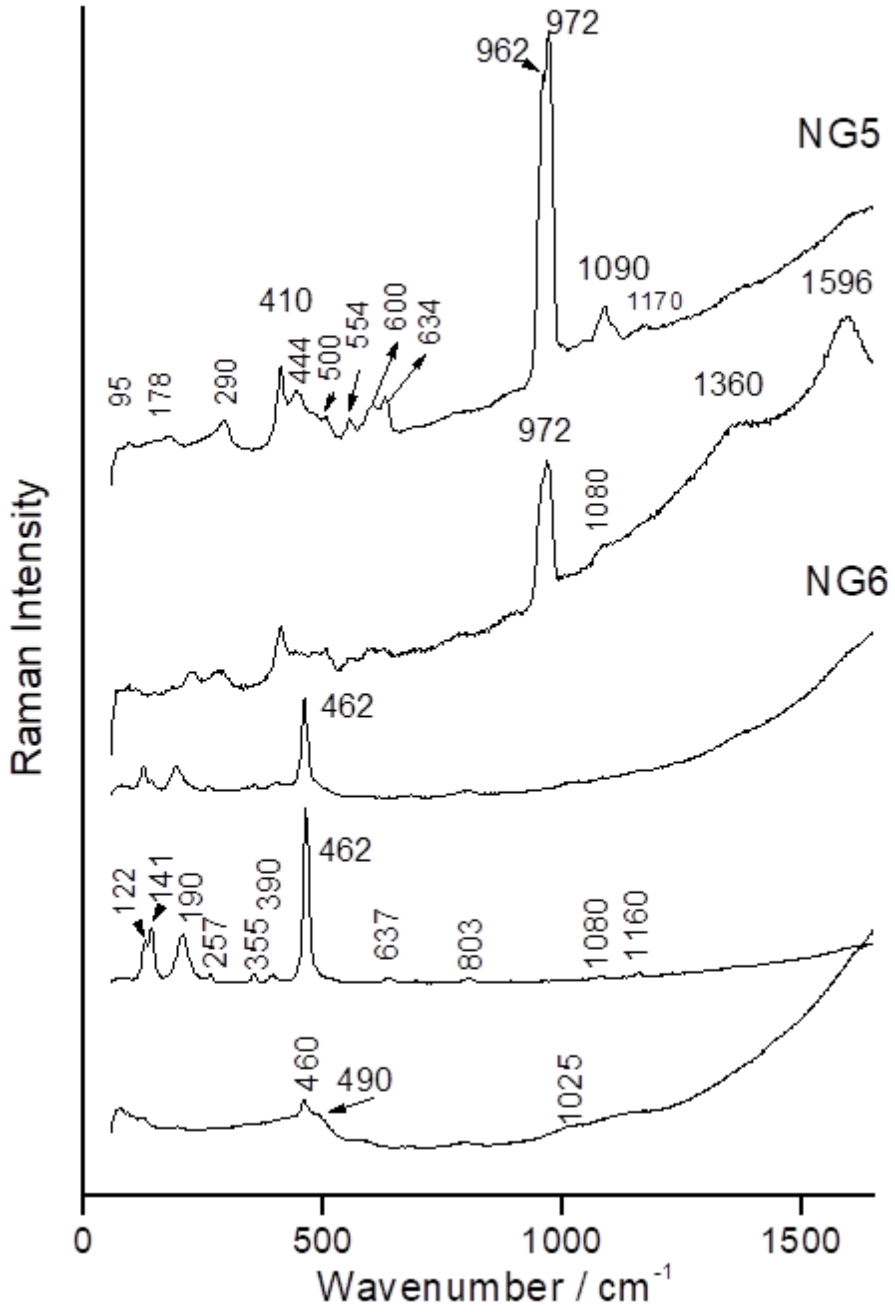

FIGURE 3 RIGHT BOTTOM

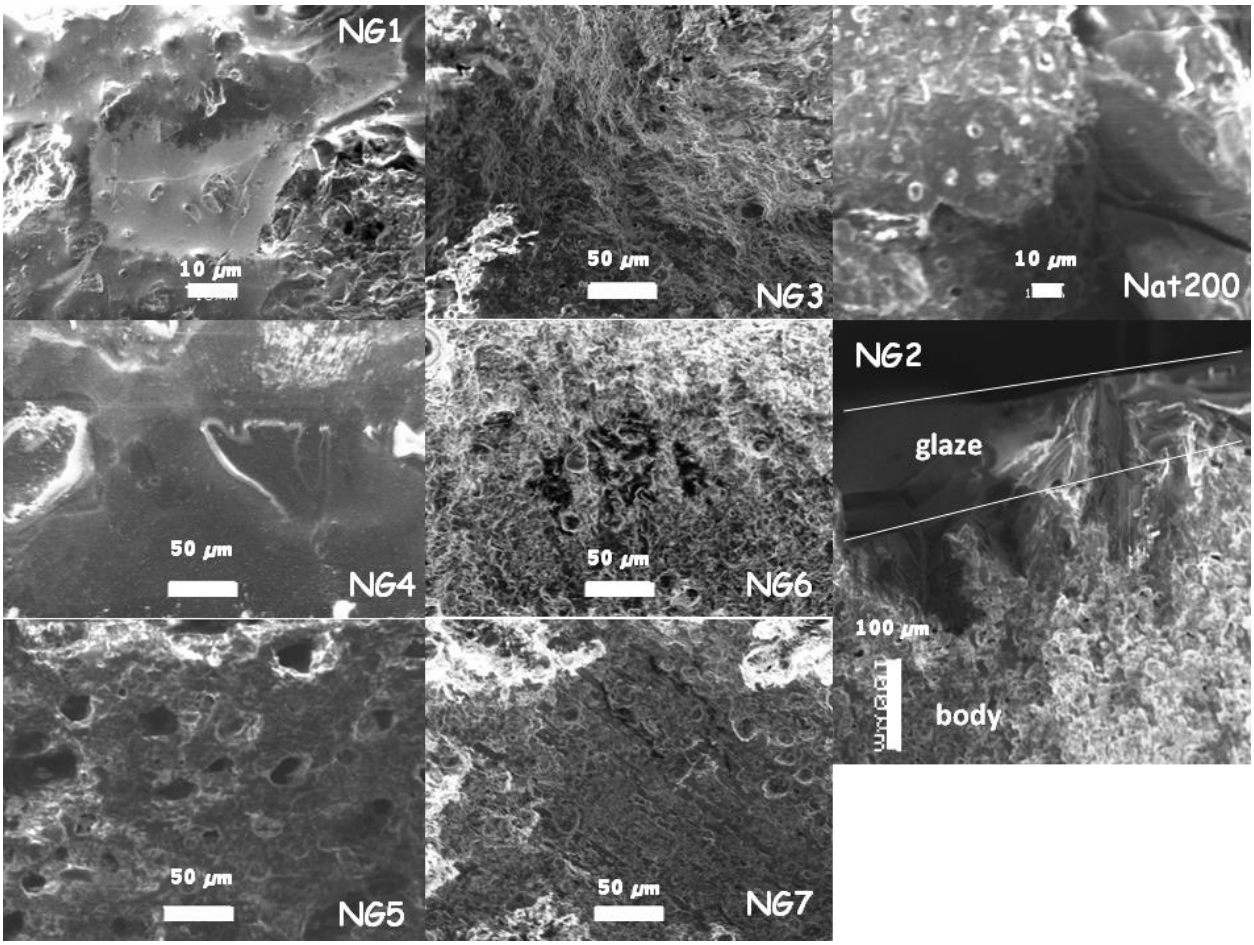
NG1
10 µm
50 µm
NG3
10 µm
Nat200
NG2
glaze
body
100 µm
50 µm
NG4
50 µm
NG6
50 µm
NG5
50 µm
NG7

FIGURE 4 TOP

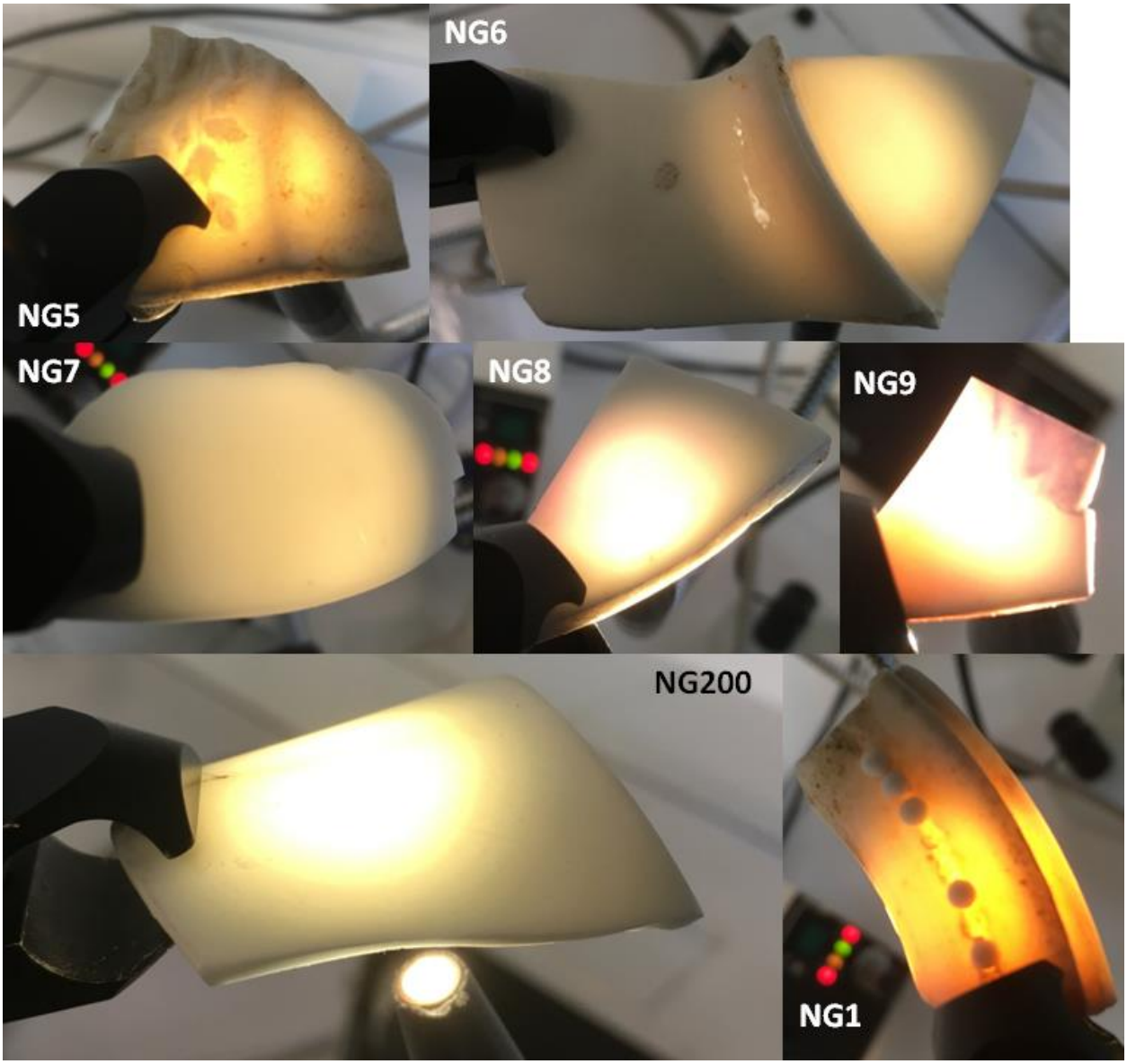

FIGURE 4 BOTTOM

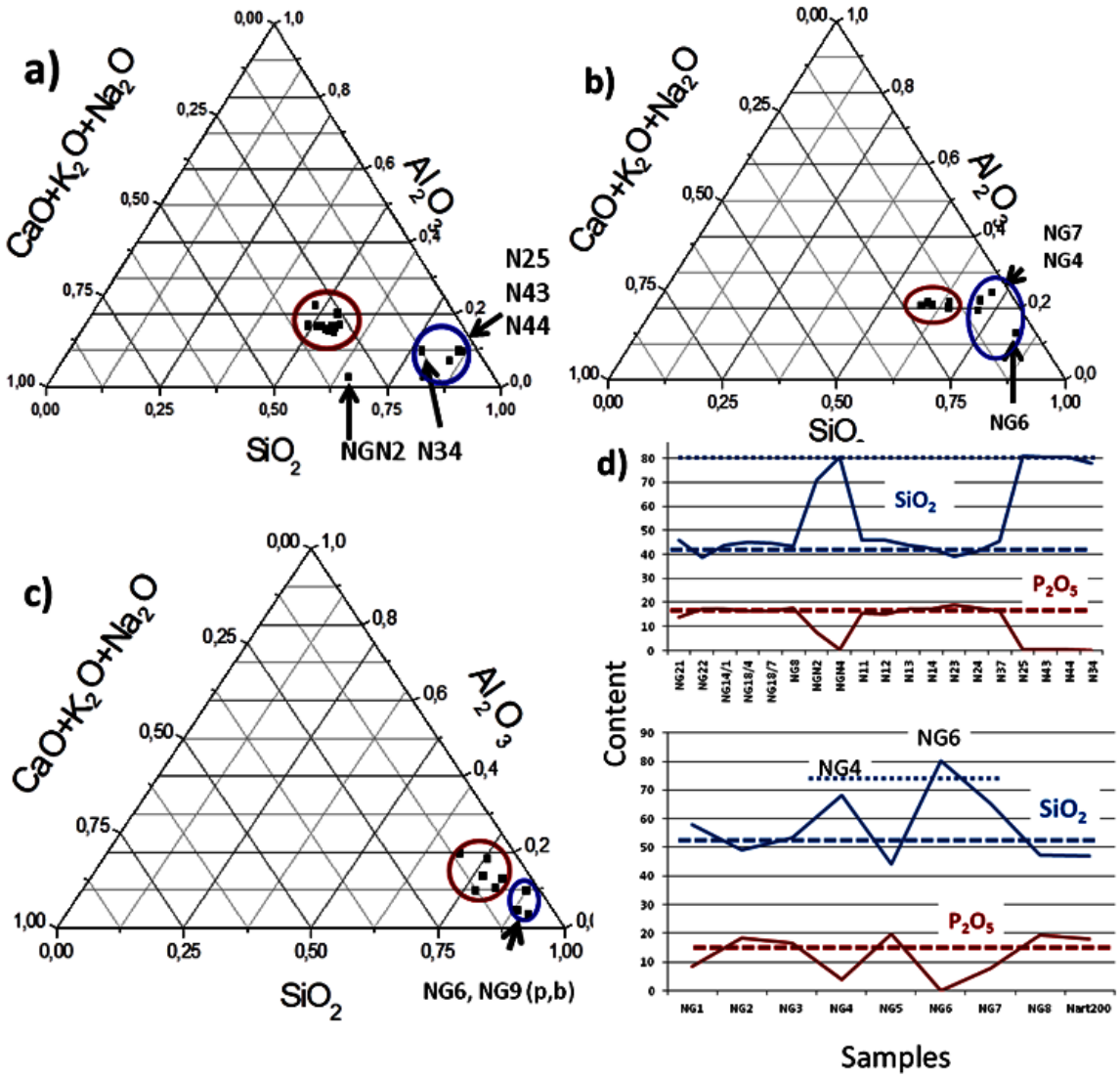
a)
b)
c)
d)
CaO+K2O+Na2O
Al2O3
SiO2
N25
N43
N44
NGN2
N34
NG7
NG4
NG6
NG6, NG9 (p,b)
P2O5
Content
Samples

FIGURE 5

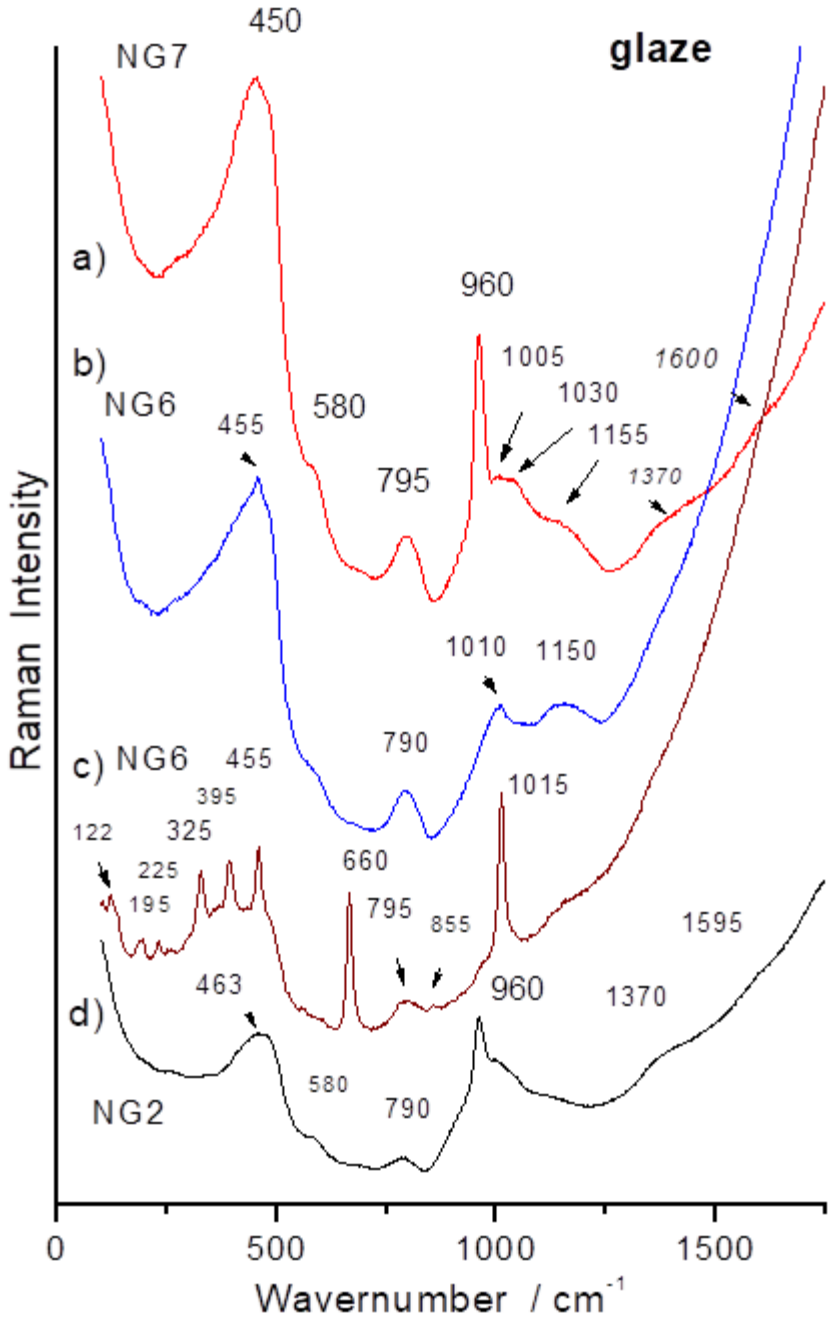
450
NG7
glaze
a)
960
b)
1005
1600
1030
NG6
455
580
1155
795
1370
1010
1150
c) NG6
455
790
395
1015
122
325
225
660
195
795
855
1595
463
960
1370
d)
580
NG2
790
Raman Intensity
0
500
1000
1500
Wavernumber / cm-1

FIGURE 6

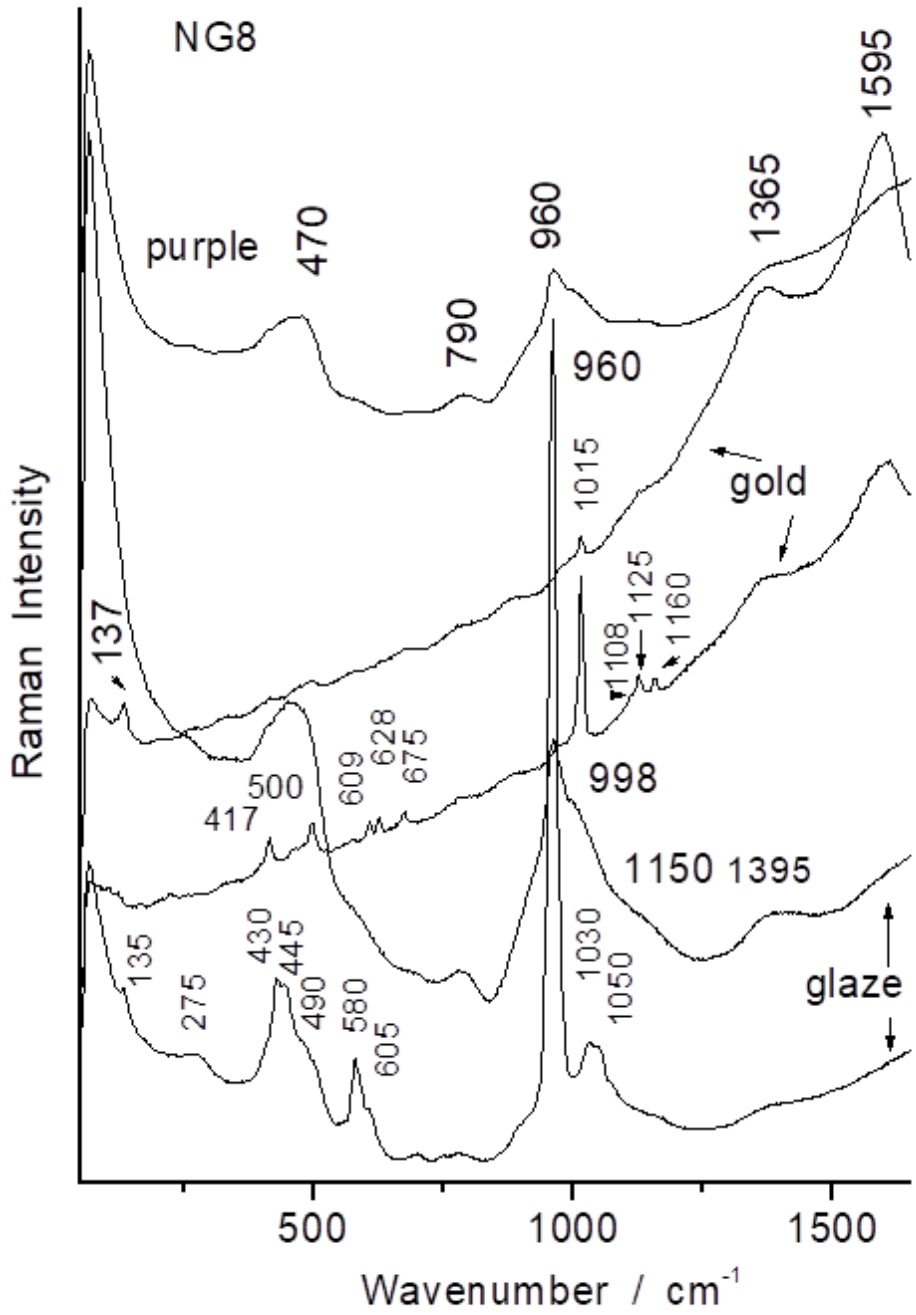

FIGURE 7 LEFT

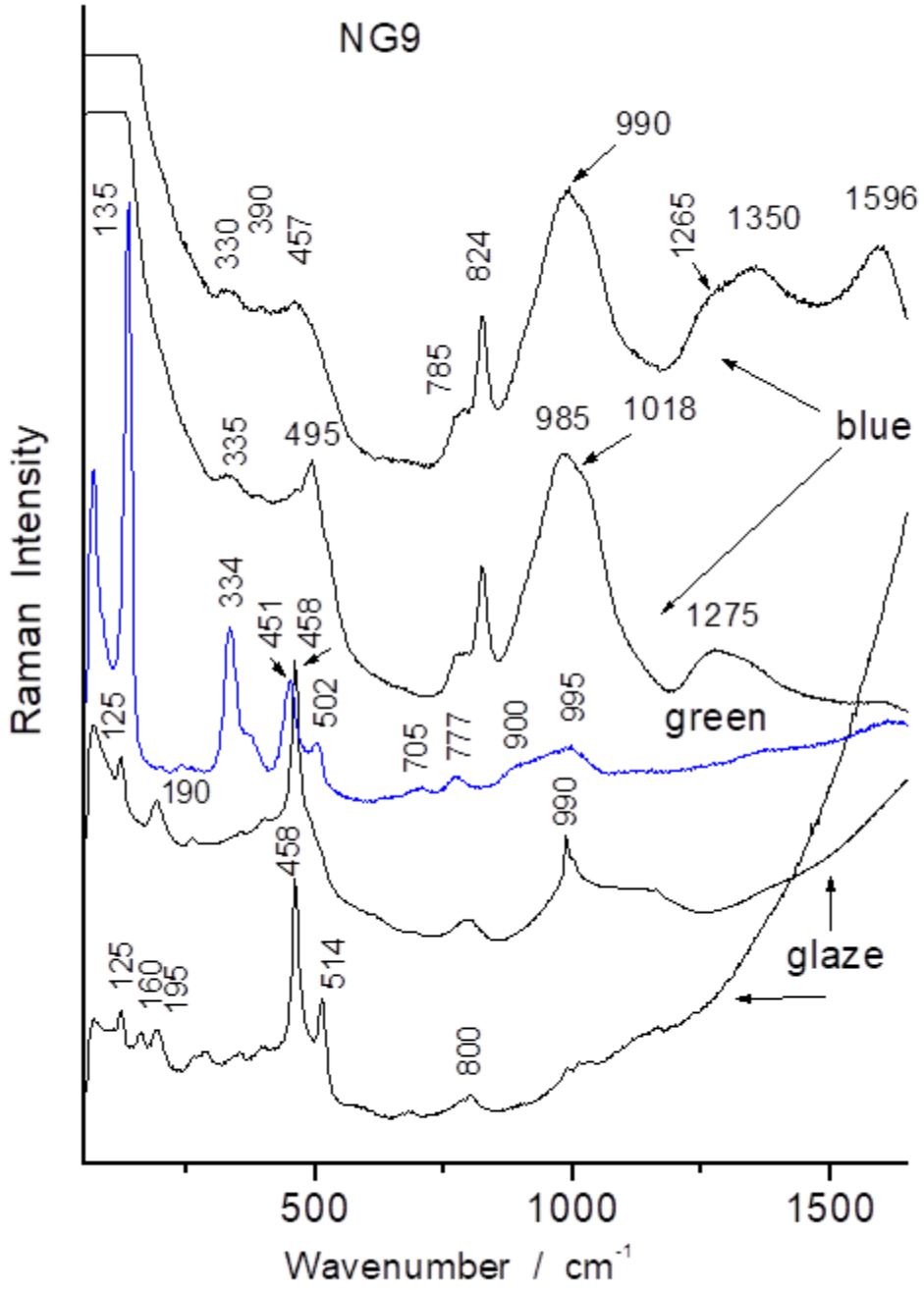

FIGURE 7 CENTER

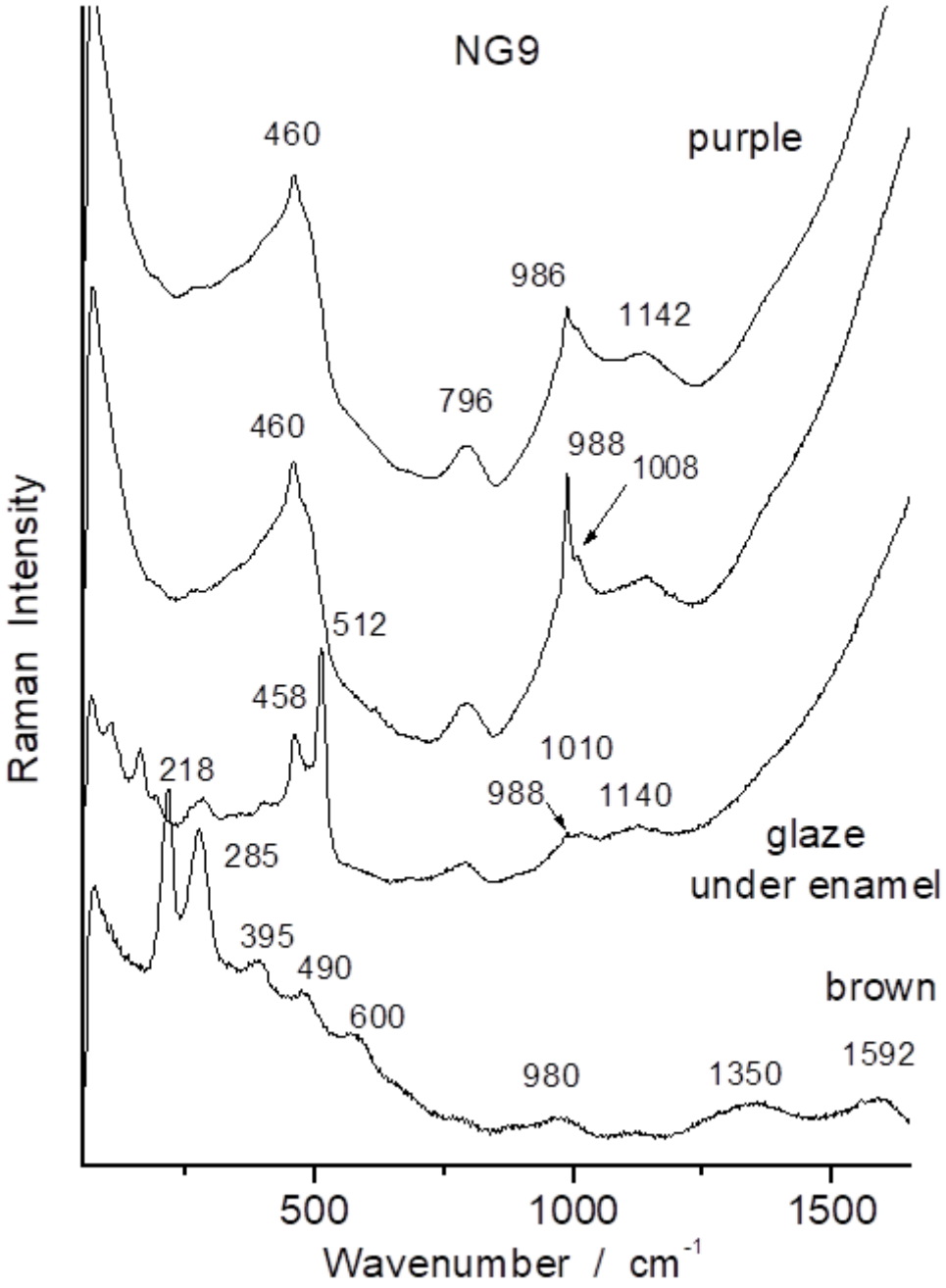

FIGURE 7 RIGHT

Table 1: Analytical data for Nantgarw porcelain (data expressed in % ages)

Analyst	Specimen	SiO_2	Al_2O_3	P_2O_5 **	CaO	MgO	Fe_2O_3	K_2CO_3	Na_2CO_3	PbO	SO_4	Equiv. BA/%
Eccles&Rackham(1922)	*NG21	46.0	17.0	13.9	19.7			2.7	0.4			35
	*NG22/*Duncombe*	38.9	18.1	17.1	22.5			2.6	0.1			40
Tite&Bimson(1991)	NG14/1	43.8	12.5	17.4	22.5	0.6		2.5	0.8			
	NG18/4	45.0	13.3	16.4	21.2	0.5	0.4	2.2	1.0			
	NG18/7	44.6	13.3	16.4	21.9	0.7	0.2	2.2	0.7			
Owen *et al*. (1998)	NG8	43.5	12.7	17.6	23.3	0.4	0.2	2.3	0.4			
	NG/N2	70.8	8.9	7.5	9.9	0.2	0.2	2.3	0.2			
	NG/N4	80.3	9.1	0.5	0.6	1.1	0.1	5.6	1.8			
Owen& Morrison (1999)	N11	45.7	13.8	15.4	21.4	0.5	0.2	1.7	0.5		0.7	
	N12	46.1	14.0	15.0	21.0	0.5	0.2	1.8	0.5		0.8	
	N13	43.7	12.7	17.1	22.9	0.4	0.2	2.4	0.4		0.2	
	N14	42.4	13.4	17.4	23.7	0.4	0.2	1.9	0.4		0.2	

Analyst	Specimen	SiO_2	Al_2O_3	P_2O_5 **	CaO	MgO	Fe_2O_3	K_2CO_3	Na_2CO_3	PbO	SO_4	Equiv. BA/%
	N23	39.0	13.3	19.1	25.5	0.4	0.2	2.0	0.4		0.1	
	N24	41.1	13.3	17.8	24.3	0.4	0.2	2.3	0.5		0.1	
	*N37	45.5	12.1	16.3	21.8	0.4	0.2	2.9	0.6		0.1	
	N25	80.7	9.0	0.5	0.5	2.2	0.1	5.4	1.5		0.1	
	N43	80.5	9.3	0.4	0.4	2.2	0.1	5.4	1.5		0.2	
	N44	80.3	9.3	0.5	0.6	1.8	0.2	5.5	1.5		0.1	
	N34	78.0	6.6		0.6	1.0		12.2	1.6			

Notes:

1. Of the nineteen specimens of Nantgarw porcelain analysed and cited in this table only three, indicated by a *, are from finished and decorated pieces, all from Museum collections.
2. Data expressed variously as H_3PO_4 (Eccles & Rackham), P_2O_5 (Tite & Bimson ; Owen & Morrison) and PO_4^{3-} (Owen *et al.*) in original reports : all have been converted to P_2O_5 figures to facilitate comparison using conversion factors described in the text.
3. Separate analyses of the glaze on the silicious sherds N25, N43 and N44 and of the specimen N37 (finished porcelain) give % PbO compositions as 15.4, 14.7 ,14.4 and 22.6 %, respectively, with an average SiO_2 content of 63.9 +/- 6.0% and Al_2O_3 of 7.5% +/- 1.5%.
4. The Nantgarw porcelain body contains no PbO, confirming that flint/lead glass cullet was not a component in the porcelain body manufacture.

Table 2: Body compositions (local: ~50x50 µm^2; error ~+- 10%).

Oxide/Sample	NG1	NG2	NG3	NG4	NG5	NG6	NG7	NG8	Nart200
SiO_2	**58.1**	**49.1**	**53.5**	**68.1**	**44.0**	**80.1**	**65.5**	**47.5**	**46.9**
Al_2O_3	**19.5**	**16.7**	**16.6**	**20.5**	**14.8**	**12.6**	**17.6**	**17.1**	**16.5**
CaO	**10.5**	**12.1**	**10.7**	**4.1**	**17.6**	**0.3**	**6.4**	**12.8**	**15.2**
P_2O_5	**8.5**	**18.5**	**16.6**	**4.0**	**19.8**	**<0.1**	**7.7**	**19.3**	**18.1**
K_2O	**2.6**	**1.4**	**1.4**	**1.9**	**1.9**	**1.2**	**0.6**	**1.3**	**0.9**
Na_2O	0.1	1.5	0.6	0.9	0.8	2.6	1.6	1.2	0.8
MgO	<0.01	0.5	0.2	0.1	0.9	3.1	-	0.5	-
Fe_2O_3	-<0.01	0.2	0.4	0.4	0.2	0.1	<0.1	0.3	0.3
PbO	-	-	-	-	-	-	-	-	0.8
Total	99.3	100	100	100	100	100.1	99.5	100	99.5
Phases (Traces)	βW CP	βW CP (Q)	βW CP Q	βW CP F	βW CP	Q	βW CP (Q)		βW CP F,(Q)
Total Flux	21.7	33.5	29.3	**10.9**	**40.1**	4.1	16.3	34.6	35

βW: $CaSiO_3$ β wollastonite ; CP : $Ca_3(PO_4)_2$ whitlockite ; Q : SiO_2 α quartz; F: feldspar; C: carbon

Table 3: Glaze/enamel compositions (local: ~50x50 µm^2; error ~+- 10%)

Sample	NG2	NG6	NG7	NG9						NG8		
Oxide				maroon	green	purple	blue	gilding	no	purple	gilding	no
SiO_2	**76.7**	**84.5**	**75.7**	67.5	77.6	86.6	86.0	32.5		70.4	33.2	66.9
Al_2O_3	**9.7**	**9.6**	**13.5**	8.8	12.3	3.4	4.5	4.8		16.8	4.8	18.7
CaO	**9.0**	**0.2**	**6.3**	3	0.8	0.6	0.9	0.8		1.1	**6.4**	**5.1**
P_2O_5	**<0.1**	**-**	**0.2**	0.4	-	-	-	-		-	-	-
K_2O	1.2	1.1	1.8	2	0.6	1.2	1.2	0.7		1.2	1.9	1.5
Na_2O	2.3	2.2	1.0	1.9	**4.1**	**3.3**	**4.8**	-		**3.5**	0.9	3.8
MgO	0.3	1.1	-	2.2	3.7	1.3	1.0	-		0.8	0.5	2.1
Fe_2O_3	0.2	0.5	0.3	**13.2**	0.2	0.3	0.1	1.1		1.4	0.7	0.3
PbO	**0.5**	**0.8**	**1.2**	0.7	0.2	**1.1**	0.2	-		**3.3**	**3.5**	1.6
CoO	-	-	-	-	-	-	**0.8**	-		-	-	-
SnO	-	-	-	0.2	-	**1.7**	-	-		-	-	-
Au	-	-	-	-	-	**0.2**	-	**60.1**		1.5	48.1	-
MnO_2	-	-	-	-	-	0.1	-	-		-	-	-
CuO	-	-	-	-	**0.3**	-	-	-		-	-	-
As_2O_5	-	-	-	-	**-**	-	0.5	-		-	-	-
Total	99.9	100	100	99.9	99.8	99.8	100	100		100	100	100
Total Flux	13	4.3	10.5	8	6.2	6.2	5.6			9.1		12
Phases (Raman)	CP	D	CP	H C	Py C	CP Q F	A C	C	Q F		αW C	

βW : $CaSiO_3$ β wollastonite ; CP : $Ca_3(PO_4)_2$ whitlockite ; Q : SiO_2 α quartz; F: feldspar; D : $MgSiO_3$ diopside ; Py: pyrochlore; H: hematite; A: Pb-As apatite; -: not measured or not detected